

# Adsorption isotherm and kinetic studies of Cr(VI) removal by a new strain of *Staphylococcus sciuri*

Jutamas Pantab<sup>a</sup>, Kanuennit Sirisom<sup>b</sup>, Jittima Charoenpanich<sup>a,b,\*</sup>

<sup>a</sup> Bioengineering Program, Faculty of Engineering, Burapha University, Chon Buri 20131 Thailand

<sup>b</sup> Department of Biochemistry, Faculty of Science, Burapha University, Chon Buri 20131 Thailand

\*Corresponding author, e-mail: jittima@go.buu.ac.th

Received 17 Sep 2021, Accepted 4 Mar 2022

Available online 25 May 2022

**ABSTRACT:** This study describes a new strain of *Staphylococcus sciuri* as a novel bacterium for Cr(VI) removal. Dried cells of the bacterium showed complete removal of 30 mg/l Cr(VI) within 9 h at 40 °C and pH 2.0. The experimental data in the Cr(VI) concentration range of 30–100 mg/l fitted well with the pseudo-second order kinetic model and Langmuir isotherm ( $R^2 = 0.9724$  and maximum adsorption capacity of 120.48 mg/g). The rate of Cr(VI) adsorption was best described by a Boyd plot and the intraparticle diffusion model. X-ray photoelectron spectroscopy suggested that *S. sciuri* used carbon and oxygen functional groups for binding Cr(VI). The quick removal of Cr(VI) in this study supports application of *S. sciuri* to reduce Cr(VI) environmental risk.

**KEYWORDS:** biosorption, Cr(VI) removal, *Staphylococcus sciuri*, adsorption kinetics, equilibrium isotherm

## INTRODUCTION

Chromium is an environmentally persistent and complex contaminant of increasing concern. The major sources of chromium released into the environment are aqueous effluents from electroplating, welding, alloy formation, leather tanning, and the electronic and metallurgy industries [1]. Chromium exists in several oxidation states. Among them, only the trivalent Cr(III) and hexavalent Cr(VI) stable oxidation forms significantly impact the environment [2]. Cr(III) is relatively water insoluble, exhibits little or no toxicity [3], and is an essential trace nutrient of living organisms [4]. By contrast, Cr(VI) typically exists as highly water-soluble and highly toxic chromate anions ( $\text{CrO}_4^{2-}$  and  $\text{Cr}_2\text{O}_7^{2-}$ ), which are poorly adsorbed by soil and organic matter [5], making them mobile in groundwater. Various concentrations of Cr(VI) have been detected in streams depending on their source. The concentration of Cr(VI) leaching from waste dumps and industrial effluents has been documented between 15 and 2500 mg/l [6]. If inappropriately managed, Cr(VI) can be easily mobilised and carried into the food web directly. At each level of the food chains, the concentration of Cr(VI) increases, resulting in biomagnification. Cr(VI) is extremely toxic, mutagenic, carcinogenic, and teratogenic to living organisms [7]. Human toxicity of Cr(VI) ranges from skin irritation to tissue injuries [8]. The WHO announced that the discharge limit for Cr(VI) in drinking water is < 0.05 mg/l, whereas < 2 mg/l is the allowable value for total chromium [9]. Thus, chromium-contaminated wastewater from industries must be managed before discharge into the environment.

Physicochemical processes, including chemical precipitation and ion exchange separation, have been adopted to reduce Cr(VI) from industrial efflu-

ents [10]. However, these methods have certain drawbacks. For instance, large inputs of energy and cost are required, and the secondary contaminants generated during the process are difficult to be removed. Adsorption is an alternative environmentally suitable method for removing Cr(VI). The usefulness of this method lies in the benefits of recovery performance and easily controlled process [11]. The major concern for the practical use of this method is operating cost. Therefore, cost-effective and practically acceptable adsorbents are needed.

Adsorption of Cr(VI) using appropriate microorganisms offers an efficient and attractive route to decrease Cr(VI) contamination [12]. This approach provides several advantages over conventional methods in terms of cost effectiveness and efficiency; it also has no toxic sludge production and is an eco-compatible means of treating industrial effluents and reclaiming land. Most studies on Cr(VI) removal focused on the genera *Bacillus* [13], *Enterobacter* [14], *Escherichia* [15], and *Pseudomonas* [16]. However, the mechanisms involved in removal are complex, and the interaction between Cr(VI) and bacterial cells is species dependent [17]. Hence, understanding the removal mechanism is the primary requisite to control the treatment. The present study introduced a new bacterium which can remove Cr(VI) in a practical manner. Continuous removal of Cr(VI) was monitored in batch operating mode. The mechanism governing Cr(VI) removal by the bacterium was studied using equilibrium isotherms and adsorption kinetics.

## MATERIALS AND METHODS

### Isolation of Cr(VI)-reducing bacterium and strain identification

The bacterium used in this study was isolated from marine sediments of Ao Prao Rayong, Thailand during

crude oil release disaster (physicochemical properties during collection; depth of 5 m, temperature of 32 °C, pH 8.8 and pressure of 1.6 atm). The strain was identified using the API skills method (API® Staph, BioMérieux, France) and based on 16S rRNA gene sequence [18]. Polymerase chain reaction (PCR) amplification of the 16S rRNA gene, sequence analysis, and construction of the phylogenetic tree were performed as described previously [19]. Sequence data were submitted to the GenBank database (accession no. KM370128).

The Cr(VI)-reducing bacterium was preliminarily screened using a chromate reductase gene. PCR amplification of the chromate reductase gene and sequence analysis were performed as described by Patra et al [20]. Thereafter, the bacterium was consequently tested for production of chromate reductase.

The bacterium was cultivated in nutrient medium at 37 °C and 250 rpm for 24 h. The cell pellet was harvested, resuspended in 200 mM phosphate buffer (pH 7.0), and then disrupted by ultrasonication for 10 min (5 s on/off pulse). The cell lysate was centrifuged at 12 000 × *g* for 15 min at 4 °C to eliminate cell debris. The protein content of the cell-free supernatant (crude enzyme solution) was determined using the Bradford method [21] with bovine serum albumin as the standard. Chromate reductase activity was measured by dichromate reduction. The reaction mixture (1 ml) was composed of Cr(VI) and nicotinamide adenine dinucleotide (NADH) at a final concentration of 100 μM in 200 mM potassium phosphate buffer (pH 7.0) and ~2 mg total protein of the crude enzyme solution. The assay mixture was incubated for 30 min at 37 °C, and the reaction was stopped by adding 0.5 ml of 20% (v/v) TCA. Then, the mixture developed a pink colour after adding double volumes of 0.5% (w/v) diphenylcarbazide in acetone. Cr(VI) was estimated using the diphenylcarbazide method [22] as described below. A set of controls was prepared in a similar manner except that the enzyme was added after adding TCA. One unit of activity of chromate reductase was defined as the amount of enzyme that reduced 1 mM of chromate per min under the assay conditions.

### Cr(VI) analysis

The amount of residual Cr(VI) was quantified using the diphenylcarbazide method [22]. A Cr(VI) standard curve was prepared with different concentrations of Cr(VI) (0–2 mg/l). The  $R^2$  value was 0.9993. The bacterial cells were removed from culture by centrifugation at 10 000 × *g* for 10 min, and Cr(VI) was measured in the supernatant. Synthetic wastewater without Cr(VI) was used as a control. The percentage of removed Cr(VI) and adsorption capacity were calculated as previously described by Cherdchoo et al [23].

### Preparation of living and dried cells

The *S. sciuri* was inoculated into nutrient medium at 37 °C and 250 rpm for 24 h. The cells were grown in the same condition to the late exponential phase. Living cells were harvested by centrifugation at 8000 rpm for 20 min at 4 °C, and the cell pellets were washed with deionized water before used for Cr(VI) adsorption. For preparing the bacterial dried cells, an appropriate amount of living cells was washed thoroughly with deionized water and kept at 60 °C for 3 days or until the weight was constant. The dried cells were blended, sieved to retain particles between 0.1–0.5 mm, and stored in a desiccator until used.

To estimate the change of culture growth, living and dried cells of *S. sciuri* were inoculated in synthetic wastewater with 30 mg/l initial Cr(VI) concentration and incubated at 40 °C for 72 h. Aliquots were taken for pH analysis, and the growth pattern was studied by the measurement of the optical density at 600 nm.

### Adsorption experiments

Adsorption of Cr(VI) onto the bacterium cell was performed in synthetic wastewater in accordance with the methods described by Kishida et al [24] and Yin et al [25] with modifications. The synthetic wastewater has a pH ranging between 6.0 and 7.0, total chemical oxygen demand (COD) of 3040 mg COD/l, soluble COD of 2960 mg COD/l, mixed liquor suspended solid (MLSS) of 3.5 mg MLSS/l, and ammonia nitrogen ( $\text{NH}_4^+\text{-N}$ ) of 34.70 mg N/l. A 6 l acrylic vessel (size: 8'' × 12'') containing 5 l of synthetic wastewater amended with initial Cr(VI) concentration (30–100 mg/l) was continuously batch-operated for 72 h at 40 °C and pH 2.0. Samples were drawn out at regular time intervals and analysed for disappearance of Cr(VI) as described above. Data with average values from the triplicate sets were reported with errors.

### Characterisation procedures

The bacterial cells before and after adsorption with 50 mg/l Cr(VI) were characterised by transmission electron microscopy-energy dispersive X-ray (TEM-EDX) and X-ray photoelectron spectroscopy (XPS). Sample preparation and analyses were performed as described previously [23]. The bacterial cells grown under similar conditions but without Cr(VI) were used as a control for comparison.

### Adsorption isotherms

Adsorption isotherms were measured against 30–100 mg/l Cr(VI) concentrations in 50 ml of synthetic wastewater (pH 2.0). Experiments were performed at 40 °C, 150 rpm, and 8 g/l bacterial biomass for 24 h to ensure that adsorption equilibrium was attained. All experiments were repeated three times, and the average values were used for analysis. The two-parameter

isotherm Langmuir and Freundlich models were selectively examined with the experimentally obtained equilibrium data based on the  $q_e$  value [26].

### Adsorption kinetic studies

Kinetic studies were used to predict the mechanism and characteristics of Cr(VI) adsorption by *S. sciuri*. In this study, classical kinetic models based on adsorption and reduction were tested to fit the experimental data. Pseudo-first-order kinetic and pseudo-second-order kinetic models [27], including an intraparticle diffusion model [28] and the Boyd model [29], were considered. All adsorption kinetic experiments were performed at 40 °C and pH 2.0. Kinetic curves were acquired at a predetermined time interval of 3 h for 24 h.

#### The pseudo-first-order kinetic model

A non-linear form of pseudo-first-order kinetic equation has been proposed as:

$$q_t = q_e (1 - e^{-k_1 t}). \quad (1)$$

The linear form of pseudo-first-order model is generally expressed as follows:

$$\log(q_e - q_t) = \log q_e - \frac{k_1}{2.303} t, \quad (2)$$

where  $q_e$  and  $q_t$  are the adsorption capacities expressed in (mg/g) at equilibrium and in a time  $t$  (min), respectively, while  $k_1$  is the pseudo-first-order rate constant.

The plots of  $\log(q_e - q_t)$  versus  $t$  shows the slope and intercept as  $k_1$  (pseudo-first-order rate constant) and  $q_e$  (equilibrium capacity), respectively [27].

#### The pseudo-second-order kinetic model

The adsorption kinetic may also be described by the pseudo-second-order model that was purposed by Ho and McKay [27]. The non-linear form of reaction is represented as follows:

$$q_t = \frac{k_2 q_e^2 t}{1 + k_2 q_e t}. \quad (3)$$

This is integrated rat law for a pseudo-second-order model chemisorption reaction (Eq. (3)) which can be rearranged as:

$$\frac{1}{q_t} = \frac{1}{k_2 q_e^2} + \frac{1}{q_e} t, \quad (4)$$

where  $q_t$  (mg/g) is the adsorption capacity at time  $t$  (min),  $q_e$  (mg/g) is the equilibrium capacity, and  $k_2$  is the pseudo-second-order rate constant.

The plot of  $1/q_t$  versus  $t$  at different Cr(VI) concentrations gives a straight line with slope of  $1/q_e$  and intercept of  $1/k_2 q_e^2$ .

#### Intraparticle diffusion model

The intraparticle diffusion is the rate-controlling step recommended for investigation [28]. This kinetic model was purposed by Weber and Morris as follows:

$$q_t = k_{id} t^{0.5} + \theta, \quad (5)$$

where  $q_t$  (mg/g) is the amount of Cr(VI) on the adsorbent surface at time  $t$  ( $\text{min}^{0.5}$ ),  $k_{id}$  is the intraparticle diffusion rate constant ( $\text{mg/g min}^{0.5}$ ), and  $\theta$  is a parameter whose value is depending on film diffusion (external diffusion) in the kinetic adsorption.

The plot of  $q_t$  versus  $t^{0.5}$  gives a straight line. The adsorption process controlled by intraparticle diffusion shows the intercept is  $\theta$ , indicating the boundary thickness layer.

#### Boyd plot

Boyd plot is typically used to confirm the role of external mass transfer during the adsorption process [29]. The model is represented as follows:

$$B_t = -0.4977 - \ln(1 - F), \quad (6)$$

where  $F$  is the fraction of solute adsorbed at time  $t$  (min) given by  $q_t/q_e$ , and  $B_t$  is the calculated value obtained from the equation.

The best fit of kinetic models to the experimental data was estimated based on the  $R^2$  values obtained from a linear plot of the equation model and Marquardt's present SD (MPSD) developed by Marquardt [30]. MPSD was calculated as reported by Cherdchoo et al [23]. A small MPSD represents an accurate estimate of  $q_t$ .

#### Statistical analysis

All experimental results were expressed as mean data from triplicate sets, considering the  $p$  value is less than 0.05 using Design-Expert 10.0. The magnitude of regression coefficient and non-linear regression analysis were obtained using Microsoft Excel program.

## RESULTS AND DISCUSSION

### Isolation and identification of Cr(VI)-reducing bacteria

Crude oil-contaminated marine sediments were cultivated on marine medium amended with  $\text{K}_2\text{Cr}_2\text{O}_7$  as the chromate source. One isolate that grew on Cr(VI) at a concentration > 30 mg/l was selected to identify the strain. The strain was a cocci-shaped, Gram-positive bacterium that reacted positively to catalase. Positive results were recorded for the test of nitrate, but results were negative for alkaline phosphatase, VP, and urea tests. Fermentation/oxidation of some substrates (D-fructose, D-glucose, D-lactose, D-maltose, D-mannitol, D-mannose, D-trehalose, D-saccharose, D-xylose, and N-acetyl-glucosamine) was detected

but did not occur with the others (D-melibiose, D-raffinose, methyl- $\alpha$ -D-glucopyranoside, xylitol, and L-arginine). The strain was classified (97.3% probability) as *Staphylococcus sciuri* according to its biochemical characteristics.

The 16S rRNA gene was sequenced and aligned using the NCBI GenBank and Ez-Taxon databases to confirm identification. A phylogenetic tree was constructed using MEGA 6.0 software and the neighbour-joining method (Fig. 1). Sequence comparisons revealed that the isolate belonged to the *Staphylococcus* genus and was most closely related to *S. sciuri*. It exhibited 99% similarity to the following *S. sciuri* strains: *S. sciuri* R10-5A (accession no. HQ154580), *S. sciuri* R1-4A (accession no. HQ154558), *S. sciuri* MBR2 (accession no. JX966420), *S. sciuri* RPa1 (accession no. JN559391), and *S. sciuri* DSM20345 (accession no. NR\_025520). Thus, this isolate was definitively identified as a new strain of *S. sciuri*, a Biosafety level 1 Risk group bacterium [31].

The identified *S. sciuri* was consequently checked for the presence of chromate reductase, an impor-

tant enzyme for Cr(VI) reduction [12]. An approximately 300 bp PCR product was cloned and sequenced. BLAST analysis showed perfect identity of the sequence obtained with the following chromate reductases: chromate reductase, Class I flavoprotein of *Escherichia coli* 1303 (accession no. CP009166.1), chromate reductase of *E. coli* BL21DE(3) (accession no. AM946981.2), and class I chromate reductase YieF of *E. coli* strain STEC367 (accession no. NZ\_CP041429.1). A full confidence level was also exhibited with the NAD(P)H-dependent chromate oxidoreductase of many *E. coli* strains: *E. coli* strain 14EC047 (accession no. NZ\_CP024155.1), *E. coli* strain 602354 (accession no. NZ\_CP025847.1), *E. coli* M8 (accession no. NZ\_CP019953.1), *E. coli* strain 120899 (accession no. NZ\_CP025916.1), and *E. coli* strain 204446 (accession no. NZ\_CP025910.1). Therefore, the expression of chromate reductase was confirmed using NADH as an electron donor [32]. Activity of  $5.66 \pm 0.81$  U/ml was detected in the crude supernatant. These results suggest that *S. sciuri* could be used as a Cr(VI) remover as evidenced by the presence of chromate reductase.

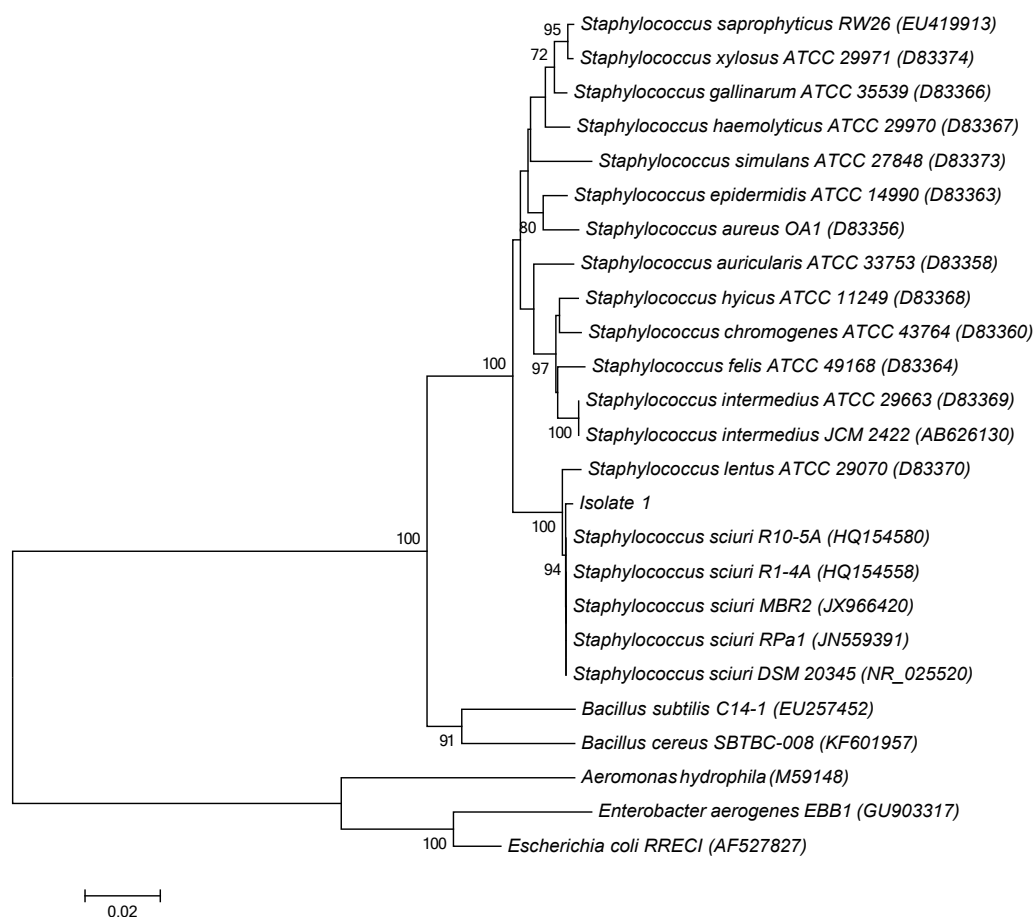


Fig. 1 Phylogenetic tree of the isolated *S. sciuri* constructed using the neighbour-joining algorithm.

### Characterisation of bacterial cells after Cr(VI) removal

XPS analysis was performed to identify the chemical changes on the cell surface of *S. sciuri* after growth in synthetic wastewater supplemented with 30 mg/l Cr(VI). The XPS survey spectra indicated that the bacterial cell surface consisted mainly of carbon (B.E. = 284.8 eV, C1s) and oxygen (B.E. = 532.8 eV, O1s). The atomic concentration percentages of carbon and oxygen decreased from 70.06% to 46.69% and from 20.76% to 14.50%, respectively, after Cr(VI) adsorption, suggesting that binding of Cr(VI) to the bacterial

cell surface occurred via carbon and oxygen functional groups, probably carboxylic, alcohol, and hydroxyl, which are easy to form complexes with chromium ions [33]. Then, the XPS spectra corresponding to the C1s and O1s narrow scan region of the bacterial cell surface with and without Cr(VI) were compared. The XPS C1s spectrum of *S. sciuri* after contact with Cr(VI) (Fig. 2a) revealed a shift in the component peaks corresponding to the hydroxy/carbonyl groups (C–O/C=O, B.E. = 288.23 eV, 12.5%) and a carboxy group (O–C=O, B.E. = 288.93 eV, 5.7%). Changes in the XPS O1s spectrum (Fig. 2b) also showed that the

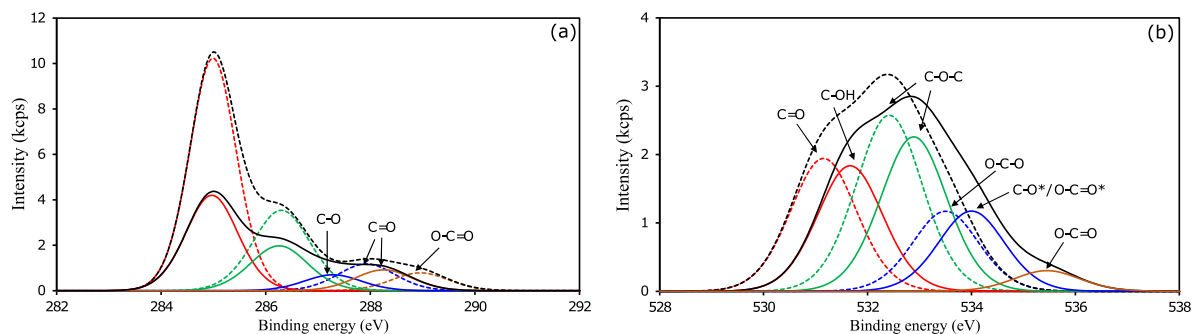


Fig. 2 Comparison of XPS spectra of *S. sciuri* before and after adsorption of Cr(VI). High-resolution spectra of (a) C1s and (b) O1s.

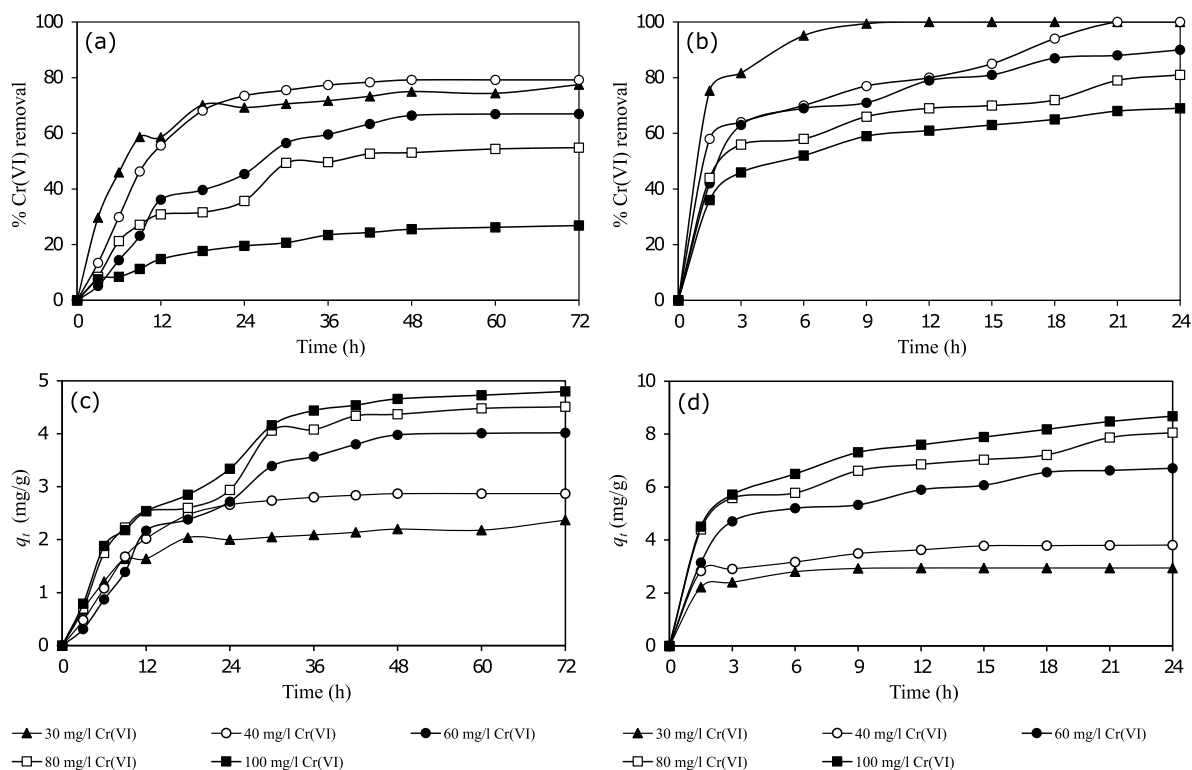
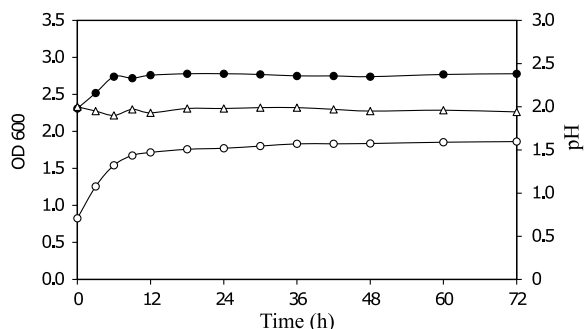


Fig. 3 Continuous operation of Cr(VI) removal by (a,c) living and (b,d) dried cells of *S. sciuri* at different initial concentrations (30–100 mg/l) at 40 °C, 150 rpm, and 8 g/l biomass dose.



**Fig. 4** Monitoring of pH (open triangle) and the growth pattern of living (open circle) and dried cells (closed circle) of *S. sciuri* under study condition.

carbon and oxygen functional groups on the surface of *S. sciuri* were associated with Cr(VI) adsorption: the carbonyl/hydroxy groups (C=O/C–OH, B.E. = 531.66 eV, 32.7%), an ether bond (C–O–C, B.E. = 532.89 eV, 40.7%), an ester bond (O–C–O/C–O\*, B.E. = 534.01 eV, 21.2%), and a carboxy group (O–C=O\*/O–C=O, B.E. = 535.46 eV, 5.4%). TEM-EDX analysis revealed the accumulation of chromium particles with 0.06 wt% within the bacterial cells treated with Cr(VI) (data not shown). These results confirm the interaction of Cr(VI) with the bacterial cell surface.

#### Adsorption isotherm and kinetic studies

Living and dried cells of *S. sciuri* were tested for the removal of different initial Cr(VI) concentrations. As shown in Fig. 3, the % Cr(VI) removal and adsorption capacity had a similar pattern, which strongly depends on the cultivation time. The removal efficiency increased continuously, and equilibrium was reached after 24 h of operation. A complete removal of 30 mg/l Cr(VI) was observed after 9 h. The dried cells of *S. sciuri* showed higher efficiency for Cr(VI) removal than the living cells. Monitoring of the cell growth pattern (Fig. 4) revealed the revival of *S. sciuri* dried cells under studied condition. This suggested that adsorption of Cr(VI) is related to cell activity together with interaction of Cr(VI) with the rehydrated biomass.

The Langmuir and Freundlich isotherm equations were used to determine the mechanism of Cr(VI) adsorption by *S. sciuri* at 40 °C. Table 1 shows the experimental data evaluated for both models. The Langmuir isotherm (Fig. 5a) provided a satisfactory fitting

of equilibrium data with high correlation coefficient ( $R^2 = 0.9724$ ). The maximum adsorption capacity ( $q_m$ ) and  $K_L$  value were estimated to be 120.48 mg/g and 0.0944 l/mg, respectively. The calculated  $R_L$  values for the adsorption of Cr(VI) on bacterial cells were 0.0961–0.2617. This range indicates the favourable adsorption of Cr(VI) by bacterial cells under the study conditions. The moderate  $R^2$  value ( $R^2 = 0.8739$ ) suggests that the Freundlich isotherm is unsuitable for Cr(VI) adsorption by this bacterium (Fig. 5b). The  $1/n$  value, which lies between 0 and 1, indicates favourable adsorption. The Freundlich isotherm constant ( $K_f$ ) was calculated to be 19.37 mg/g. A comparative plot of experimental and calculated adsorption capacity values (Fig. 5c) revealed that the Langmuir isotherm model described the adsorption of Cr(VI) onto *S. sciuri* better than the Freundlich isotherm model, indicating that Cr(VI) uptake occurs on heterogeneous surfaces by monolayer adsorption [23]. Previous document showed that Cr(VI) adsorption capacity of dried *S. aureus* was 27.36 mg/g [34]. Another research also suggests that the Cr(VI) adsorption capacity was 43.48 mg/g for *S. xylosus* [35]. Our study presented that the dried cells of *S. sciuri* (120.48 mg/g of adsorption capacity) were more effective for Cr(VI) removal than other *Staphylococcus* strains previously published. Thus, this well supported the application of *S. sciuri* dried cell as an adsorbent agent for Cr(VI) removal.

The experimental data were analysed with pseudo-first-order and pseudo-second-order kinetic models to understand the kinetics of Cr(VI) adsorption. Table 2 lists the kinetic constants as well as  $R^2$  and MPSD values representing the closeness of the values between the experimental and calculated adsorption capacities. After fitting the experimental data to the pseudo-first-order (Fig. 6a,d) and pseudo-second-order kinetic (Fig. 6b,e) models, results showed that the latter describes Cr(VI) adsorption kinetics better than the former. The  $R^2$  values obtained from the linear plots of the pseudo-second-order kinetic model (Fig. 6b) were closer to unity than those obtained from the pseudo-first-order plots (Fig. 6a and Table 2). The adsorption capacities ( $q_t$ ) calculated by the model were close to those determined experimentally. These findings were confirmed by low MPSD values. These data suggest that adsorption of Cr(VI) onto the cell surface of *S. sciuri* is consistent with a pseudo-second-order kinetic model. Hence, we can assume that the sorption rate is controlled by chemical interactions.

**Table 1** Isotherm parameters for Cr(VI) adsorption by *S. sciuri*.

$K_L$ (calculated) (l/mg)	Langmuir parameter			$R^2$	$K_f$ (calculated) (mg/g)	Freundlich parameter		$R^2$
	$R_L$ (l/mg)	$q_m$ (mg/g)				$1/n$	$n$	
0.0944	0.0961–0.2617	120.48		0.9724	19.37	0.19	5.097	0.8739

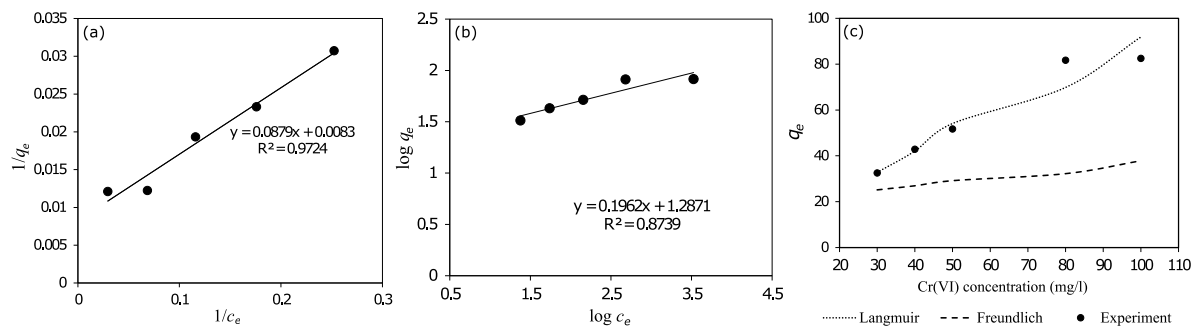


**Fig. 5** (a) Langmuir isotherm, (b) Freundlich isotherm, and (c) comparative plots of experimental and calculated adsorption capacity values for Cr(VI) adsorption by *S. sciuri* at 30–100 mg/l Cr(VI). Experimental conditions: 40 °C, 8 g/l biomass dose, pH 2.0, and 150 rpm.

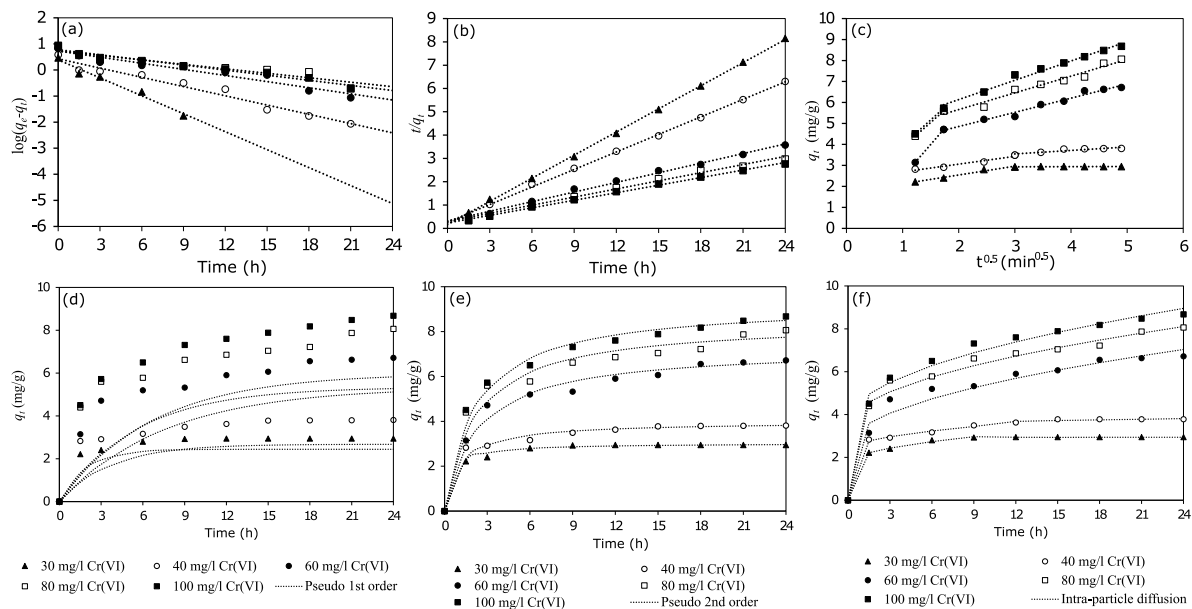


**Fig. 6** Linear and non-linear plots for the adsorption kinetic studies of Cr(VI) by *S. sciuri* at 30–100 mg/l Cr(VI). (a,d) Pseudo-first-order model; (b,e) pseudo-second-order model; and (c,f) intraparticle diffusion model. Symbols represent the experimental data, and dotted lines imply theoretical data fitting of the model. Experimental conditions: pH 2.0, 150 rpm agitation speed, 40 °C, and 8 g/l biomass dose.

An intraparticle diffusion model was also tested to predict the diffusion mechanism. Fig. 6f is a  $q_t$  plot against time of the diffusion model. The linear portion of the  $q_t$  vs  $t^{0.5}$  plots (Fig. 6c) for the adsorption of Cr(VI) onto bacterial surfaces did not pass through the origin, indicating that pore diffusion was not the only rate-controlling step. Two linear portions were identified, suggesting that the adsorption process follows two steps. The  $k_{id}$  values at the different initial Cr(VI) concentrations were calculated from the slopes of the respective plots at each stage (Table 2). This finding can be attributed to the adsorption of Cr(VI) following the boundary layer diffusion effect at the initial stage and the intraparticle diffusion effect at the next stage.

A Boyd plot was consequently used to predict the

slow step in adsorption. If the plot is linear and passes through the origin, then adsorption is driven by particle diffusion; otherwise, it is controlled by film diffusion [36]. Fig. 7 shows that the plots were linear but did not pass through the origin, indicating that film diffusion controlled the adsorption at the studied concentrations. Together with the results obtained above, intraparticle diffusion and film diffusion play roles in the adsorption of Cr(VI) by *S. sciuri*.

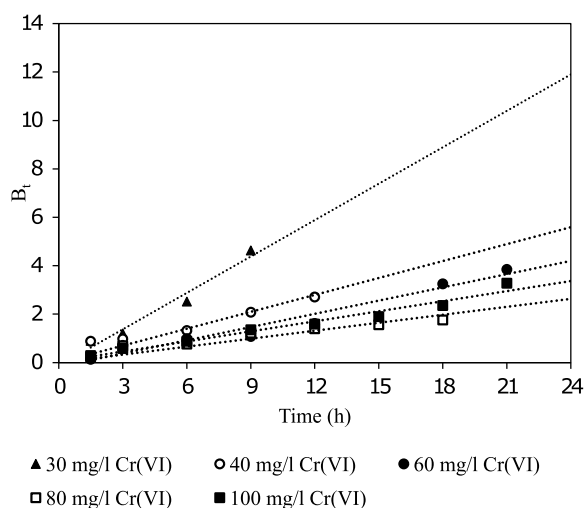
In sum, this paper proposes the following Cr(VI) removal mechanism by *S. sciuri*. Cr(VI) initially migrates from the solution to the cell surface. Then, it attaches to the cell through chemical interactions possibly by the carboxyl/carbonyl/hydroxy groups on the cell surface. Monolayer adsorption in the film covering

**Table 2** Kinetic constants for Cr(VI) adsorption by *S. sciuri*.

Experimental		Kinetic model constant, $R^2$ , and MPSD							
Cr(VI) (mg/l)	$q_{t,exp}$ (mg/g)	Pseudo-first-order adsorption				Pseudo-second-order adsorption			
		$q_{t,calc}$ (mg/g)	$k_1$ ( $\text{min}^{-1}$ )	$R^2$	MPSD	$q_{t,calc}$ (mg/g)	$k_2$ ( $\text{min}^{-1}$ )	$R^2$	MPSD
30	2.95	2.44	0.529	0.976	28.13	2.96	0.651	1.000	3.73
40	3.81	2.68	0.272	0.965	51.66	3.82	0.231	0.999	8.73
60	6.71	5.28	0.180	0.937	44.31	6.63	0.059	0.995	8.62
80	8.06	5.12	0.131	0.879	65.81	7.75	0.053	0.991	12.62
100	8.68	5.82	0.150	0.960	60.28	8.50	0.050	0.997	8.32

Cr(VI) (mg/l)	$q_{t,calc}$ (mg/g)	Intraparticle diffusion					Boyd plot		
		$k_{id1}$ ( $\text{min}^{-1}$ )	$\theta$	$R^2$	$k_{id2}$ ( $\text{min}^{-1}$ )	$\theta$	$R^2$	MPSD	$R^2$
30	2.94	0.420	1.704	0.980	0.007	2.914	0.488	1.34	0.966
40	3.81	0.372	2.318	0.952	0.166	3.052	0.821	1.97	0.958
60	7.04	3.090	0.641	1.000	0.675	3.504	0.975	10.11	0.957
80	8.11	3.090	0.641	1.000	0.796	4.069	0.963	5.50	0.957
100	8.96	2.397	1.572	1.000	0.920	4.298	0.982	5.96	0.968

**Fig. 7** Boyd plot for Cr(VI) removal by *S. sciuri*. Experimental conditions: pH 2.0, 150 rpm agitation speed, 40 °C, and 8 g/l biomass dose.

the bacterial cell surface occurs, and the chromium ions are transported from the bacterial cell surface to the interior pores of the cell particles. Finally, the chromium ions accumulate intracellularly and are reduced to other forms.

## CONCLUSION

Dried cells of *S. sciuri* showed complete removal of 30 mg/l Cr(VI) within 9 h at pH 2.0 and 40 °C with a maximum adsorption capacity of 120.48 mg/g. TEM-EDX and XPS analyses showed that Cr(VI) was adsorbed on the bacterial surface using carbon and oxygen functional groups and uptake into the cell. Adsorption isotherm and kinetic studies indicated the monolayer chemisorption in film covering the bacterial cell surface. Thereafter, the Cr(VI) ions were

transported into the bacterial cell by pore diffusion mechanism, accumulated intracellularly and reduced to other forms.

**Acknowledgements:** This research was supported to JC by a Research Grant from the National Research Council of Thailand through Burapha University (Grant no. 204/2561). We also thank the Faculty of Engineering, Burapha University for the graduate research assistant scholarship awarded to JP. We would like to thank Dr. Jariyawadee Suriyaphan for sampling of the marine sediments used in this study.

## REFERENCES

- Mohan D, Pittman CU (2006) Activated carbons and low cost adsorbents for remediation of tri- and hexavalent chromium from water. *J Hazard Mater* **137**, 762–811.
- Richard FC, Bourg ACM (1991) Aqueous geochemistry of chromium: a review. *Water Res* **25**, 807–816.
- Nriagu JO, Nieboer E (1988) *Chromium in the Natural and Human Environments*, Wiley-Interscience, New York, USA.
- Whitacre DM (2012) *Reviews of Environmental Contamination and Toxicology*, Springer Nature, Switzerland.
- Krishnani KK, Ayyappan S (2006) Heavy metals remediation of water using plants and lignocellulosic agrowaste. *Rev Environ Contam Toxicol* **188**, 59–84.
- Liu C-C, Wang M-K, Chiou C-S, Li Y-S, Lin Y-A, Huang SS (2006) Chromium removal and sorption mechanism from aqueous solutions by wine processing waste sludge. *Ind Eng Chem Res* **45**, 8891–8899.
- IARC (1987) Monographs on the evaluation of carcinogenic risks to humans: overall evaluation of carcinogenicity. *An updating of IARC Monographs*, France.
- Cieslak-Golonka M (1995) Toxic and mutagenic effects of chromium (VI): A review. *Polyhedron* **15**, 3667–3689.
- WHO (2003) [https://www.who.int/water\\_sanitation\\_health/dwq/chemicals/chromium.pdf](https://www.who.int/water_sanitation_health/dwq/chemicals/chromium.pdf).
- Barrera-Díaz CE, Lugo-Lugo V, Bilyeu B (2012) A review of chemical, electrochemical and biological methods for aqueous Cr(VI) reduction. *J Hazard Mater* **223**, 1–12.
- Atar N, Olgun A, Wang S (2012) Adsorption of cadmium(II) and zinc(II) on boron enrichment process

- waste in aqueous solutions: Batch and fixed-bed system studies. *Chem Eng J* **192**, 1–7.
12. Thatoi H, Das S, Mishra J, Rath BP, Das N (2014) Bacterial chromate reductase, a potential enzyme for bioremediation of hexavalent chromium: a review. *J Environ Manage* **146**, 383–399.
  13. Garbisu C, Alkorta I, Llama MJ, Serra JI (1998) Aerobic chromate reduction by *Bacillus subtilis*. *Biodegradation* **9**, 133–141.
  14. Wang P-C, Mori T, Komori K, Sasatsu M, Toda K, Ohtake H (1989) Isolation and characterization of an *Enterobacter cloacae* strain that reduces hexavalent chromium under anaerobic conditions. *Appl Environ Microbiol* **55**, 1665–1669.
  15. Wang Y-T, Shen H (1997) Modelling Cr(VI) reduction by pure bacterial cultures. *Water Res* **31**, 727–732.
  16. Bopp LH, Ehrlich HL (1988) Chromate resistance and reduction in *Pseudomonas fluorescens* strain LB300. *Arch Microbiol* **150**, 426–431.
  17. Camargo FAO, Bento FM, Okeke BC, Frankenberger WT (2003) Chromate reduction by chromium-resistant bacteria isolated from soils contaminated with dichromate. *J Environ Qual* **32**, 1228–1233.
  18. Weisburg WG, Barns SM, Pelletier DA, Lane DJ (1991) 16S ribosomal DNA amplification for phylogenetic study. *J Bacteriol* **173**, 697–703.
  19. Charoenpanich J, Soongrungrong T, Chinnasri S, Suebchuea N, Suppoontong M, Thiemsawait S (2018) A novel broad-temperature active and solvent stable esterase from a newly isolated *Bacillus aerophilus*. *Biocat Agri Biotechnol* **13**, 116–122.
  20. Patra RC, Malik S, Beer M, Megharaj M, Naidu R (2010) Molecular characterization of chromium(VI) reducing potential in Gram positive bacteria isolated from contaminated sites. *Soil Biol Biochem* **42**, 1857–1863.
  21. Bradford MM (1976) A rapid and sensitive method for the quantitation of microgram quantities of protein utilizing the principle of protein-dye binding. *Anal Biochem* **72**, 248–254.
  22. APHA-AWWA-WEF (2005) *Standard Methods for the Examination of Water and Wastewater*, 21st edn, American Public Health Association–American Water Works Association–Water Environment Federation, Washington, D.C.
  23. Cherdchoo W, Nithettham S, Charoenpanich J (2019) Removal of Cr(VI) from synthetic wastewater by adsorption onto coffee ground and mixed waste tea. *Chemosphere* **221**, 758–767.
  24. Kishida N, Kim J, Tsuneda S, Sudo R (2006) Anaerobic/oxic/anoxic granular sludge process as an effective nutrient removal process utilizing denitrifying polyphosphate-accumulating organisms. *Water Res* **40**, 2303–2310.
  25. Yin Q, Miao J, Li B, Wu G (2017) Enhancing electron transfer by ferroferric oxide during the anaerobic treatment of synthetic wastewater with mixed organic carbon. *Int Biodeterior Biodegradation* **119**, 104–110.
  26. Keereerak A, Chimpa W (2020) A potential biosorbent from *Moringa oleifera* pod husk for crystal violet adsorption: Kinetics, isotherms, thermodynamic and desorption studies. *ScienceAsia* **46**, 186–194.
  27. Qiu H, Lv L, Pan B-C, Zhang Q-J, Zhang W-M, Zhang Q-X (2009) Critical review in adsorption kinetic models. *J Zhejiang Univ Sci A* **10**, 716–724.
  28. Hameed BH, Ahmad AA (2009) Batch adsorption of methylene blue from aqueous solution by garlic peel, an agricultural waste biomass. *J Hazard Mater* **164**, 870–875.
  29. Boyd GE, Adamson AW, Myers JrLS (1947) The exchange adsorption of ions from aqueous solutions by organic zeolites, II: kinetics. *J Am Chem Soc* **69**, 2836–2848.
  30. Marquardt DW (1963) An algorithm for least-squares estimation of nonlinear parameters. *SIAM J Appl Math* **11**, 431–441.
  31. US Department of Health and Human Services (2020) *Biosafety in Microbiological and Biomedical Laboratories*, 6th Edn, HHS Publication No. (CDC) 300859, Centers for Disease Control and Prevention, National Institutes of Health, USA.
  32. Sau GB, Chatterjee S, Mukherjee SK (2010) Chromate reduction by cell-free extract of *Bacillus firmus* KUCr1. *Pol J Microbiol* **59**, 185–190.
  33. Li X, Cao J, Zhang W (2008) Stoichiometry of Cr(VI) immobilization using nanoscale zerovalent iron (nZVI): a study with high-resolution X-ray photoelectron spectroscopy (HR-XPS). *Ind Eng Chem Res* **47**, 2131–2139.
  34. Wang XS, Li Y, Huang LP, Chen J (2010) Adsorption of Cr(VI) from aqueous solutions by *Staphylococcus aureus* biomass. *Clean Soil Air Water* **38**, 500–505.
  35. Aryal M, Ziagova M, Liakopoulou-Kyriakides M (2011) Comparison of Cr(VI) and As(V) removal in single and binary mixtures with Fe(III)-treated *Staphylococcus xylosum* biomass: Thermodynamic studies. *Chem Eng J* **169**, 100–106.
  36. Rorrer GL, Hsien T (1993) Synthesis of porous-magnetic chitosan beads for removal of cadmium ions from wastewater. *Ind Eng Chem Res* **32**, 2170–2178.